

Supporting information

for

Designing Dihydrofolate Reductase Inhibitors as X-ray Radiosensitizer to Reverse Radioresistance of Cervical Cancer

Yuanwei Liang^{#a}, Delong Zeng^{#a}, Yuanyuan You^{ab}, Bin Ma^a, Xiaoling Li^{ac},
Tianfeng Chen^{*a}

^a The First Affiliated Hospital, and Department of Chemistry, Jinan University, Guangzhou 510632, China.

^b Shenzhen Agricultural Product Quality and Safety Inspection and Testing Center (Guangdong Provincial Key Laboratory of Supervision and Administration of Edible Agricultural products, Market Supervision Administration), Shenzhen, China

^c Institute of Food Safety and Nutrition, Jinan University, Guangzhou 510632, China.

Supplementary Information Contents

- Experimental Section
 - Materials
 - Synthesis and Characterization
 - Cell culture
 - X-ray irradiation
 - In vitro DHFR Inhibition Assay
 - Subcellular localization
 - Wound-healing assay
 - Antiproliferative Activity
 - Cellular uptake
 - Intracellular ROS lever

- Flow cytometric analysis
 - Mitochondrial Morphology
 - Mitochondrial Membrane Potential ($\Delta\Psi$ m)
 - Caspases activity assay
 - Western blot analysis
 - *In vivo* anti-tumor analysis
 - Pathology analysis
 - Hematology analysis of HeLa xenograft nude mice
 - Pharmacokinetics analysis
 - Statistical analysis
- References
 - Synthetic route of Compounds
 - Supplementary figures

Experimental Section

Materials

Chemicals including 2,4,5,6-Tetraaminopyrimidine sulfate salt and diketones were purchased from Shanghai Macklin Biochemical Co., Ltd. HeLa cervix carcinoma cells and E6D7 normal cervical cells were purchased from American Type Culture Collection (ATCC).

Synthesis and Characterization

The schematic route for the synthesis of 2,4-diaminopteridine derivatives were showed in scheme1 (supporting information). Commercially available 2,4,5,6-Tetraaminopyrimidine sulfate salt was utilized as starting material. 2,4,5,6-Tetraaminopyrimidine sulfate salt (119 mg, 0.5 mmol) was suspended in 20 ml distilled water, NaOH (42 mg, 1.05mmol) was added. The mixture was allowed to stirred for 40 min at 50°C, an ethanol solution of different substituted ethane-1,2-dione (0.49 mmol) was added and reflux for 3h. The resulting suspension liquid was filtered and the residue was washed with distilled water (3×30 ml) and cold ethyl alcohol (2×30 ml) to afford 2,4-diaminopteridine derivatives after vacuum dried.

The Characterization spectra including HRMS, ¹H NMR ¹³C NMR were displayed in Figure S1-S17.

Acenaphtho[1,2-g]pteridine-9,11-diamine (2a), Yellow solid, 112 mg, yield: 78%. ¹H NMR (DMSO-*d*₆, 500 MHz): δ 6.67 (s, 2H), 7.66 (s, 2H), 7.93 (m, 2H), 8.19 (dd, 2H), 8.31 (dd, 2H). ¹³C NMR (DMSO-*d*₆, 125 MHz): δ 163.64, 162.89, 158.87, 155.30, 146.68, 134.51, 131.31, 131.25, 131.17, 129.88, 129.50, 129.38, 129.15, 123.67, 121.61, 119.81. Mass spectrometry (HR-MS, m/z): (M + H⁺) calcd for C₁₆H₁₁N₆ 287.1045; found 287.1033.

Phenanthro[9,10-g]pteridine-11,13-diamine (2b): Yellow solid, 123 mg, yield: 79%. ¹H NMR (DMSO-*d*₆, 500 MHz): δ 6.88 (s, 2H), 7.82-7.73 (m, 3H), 7.91-7.86 (m, 1H), 7.97 (s, 1H), 8.37 (s, 1H), 8.82-8.75(m, 2H), 9.12 (dd, 1H), 9.40 (m, 1H). ¹³C NMR (DMSO-*d*₆, 125 MHz): δ 164.05, 163.49, 155.12, 145.76, 135.39, 132.57, 131.16, 130.35, 130.01, 129.76, 129.31, 128.39, 126.22, 125.75, 124.27, 123.93, 123.68. Mass spectrometry (HR-MS, m/z): (M + H⁺) calcd for C₁₈H₁₃N₆ 313.1202; found 313.1190.

Pteridino[6,7-f][1,10]phenanthroline-11,13-diamine (2c): Yellow solid, 118 mg, yield: 75%. ¹H NMR (DMSO-*d*₆, 500 MHz): δ 7.03 (s, 2H), 7.94-7.85 (m, 2H), 8.07 (s, 1H), 8.53 (s, 1H), 9.10 (d, 1H), 9.20 (d, 1H), 9.38 (d, 1H), 9.72 (d, 1H). Mass spectrometry (HR-MS, m/z): (M + H⁺) calcd for C₁₆H₁₁N₈ 315.1093; found 315.1107.

6,7-diphenylpteridine-2,4-diamine (2d): Yellow solid, 107 mg, yield: 68%. ¹H NMR (DMSO-*d*₆, 500 MHz): δ 6.70 (s, 2H), 7.47-7.29 (m, 10H), 7.70 (s, 2H). ¹³C NMR (DMSO-*d*₆, 125 MHz): δ 163.80, 163.25, 157.76, 154.79, 145.27, 139.39, 138.98, 130.08, 129.98, 129.30, 128.47, 128.34, 121.15. Mass spectrometry (HR-MS, m/z): (M + H⁺) calcd for C₁₈H₁₅N₆ 315.1358; found 315.1361

6,7-di(furan-2-yl)pteridine-2,4-diamine (2e): Yellow solid, 62 mg, yield: 42%. ¹H NMR (DMSO-*d*₆, 500 MHz): δ 6.60 (dd, 1H), 6.66 (m, 2H), 6.78 (s, 1H), 6.82 (dd, 1H), 6.82 (dd, 1H), 7.66 (dd, 1H), 7.78 (dd, 2H), 7.85 (dd, 1H). ¹³C NMR (DMSO-*d*₆, 125 MHz): δ 164.09, 162.89, 154.80, 151.23, 150.99, 146.91, 145.67, 143.80, 134.38, 120.99, 113.87, 112.65, 112.21, 111.28. Mass spectrometry (HR-MS, m/z): (M + H⁺) calcd for C₁₄H₁₁N₆O₂ 295.0943; found 295.0933.

6,7-di(thiophen-2-yl)pteridine-2,4-diamine (2f): Yellow solid, 90mg, yield: 55%. ¹H NMR (DMSO-*d*₆, 500 MHz): δ 6.76 (s, 2H), 6.99 (dd, 1H), 7.07-7.04 (m, 1H), 7.16-7.13 (m, 1H), 7.30 (dd, 1H), 7.55 (s, 1H), 7.74 (m, 3H). ¹³C NMR (DMSO-*d*₆, 125 MHz): δ 163.62, 162.75, 154.29, 151.36, 141.50, 140.35, 138.55, 131.30, 130.14, 129.11, 128.74, 128.47, 128.08, 120.54. Mass spectrometry (HR-MS, *m/z*): (M + H⁺) calcd for C₁₄H₁₁N₆S₂ 327.0487; found 327.0487.

Cell culture

The HeLa cells were cultured in DMEM medium, supplemented with 10% FBS, 0.1% penicillin and streptomycin in a humidified incubator of 5% CO₂ at 37 °C.

X-ray irradiation

Cultured cells were irradiated with a total dose of 4 Gy, at a dose rate of 2 Gy/min at a focus surface distance of 50 cm using an Elekta Precise linear accelerator machine at room temperature.

***In vitro* DHFR Inhibition Assay**

The dihydrofolate reductase inhibition assay was performed according to the procedure using the DHFR assay kit (Sigma product code CS0340) ¹. In 96-well plate containing a solution of 20 μM dihydrofolate (DHF), 5 × 10⁻² units of recombinant human DHFR and different concentrations of the 2,4-diaminopteridine derivatives in 0.05 M phosphate buffer (containing 2% DMF), a final concentration of 200 μM NADPH was added to initiate the systematic reaction. The consumption of NADPH with conversion of DHF to THF was monitored by taking absorbance readings at 340 nm. The inhibition rate of enzymatic activity was calculated out after neglecting effects of folate, NADPH and solvent. IC₅₀ was calculated by plotting a graph between inhibition rate and the corresponding concentration of the 2,4-diaminopteridine derivatives. The inhibitory rate at different concentration of inhibitor was calculated by using the formulas as followed:

$$\text{Inhibition (\%)} = 100 - \frac{\text{Slope}_{\text{compound}} - \text{Slope}_{\text{blank}}}{\text{Slope}_{\text{control}} - \text{Slope}_{\text{blank}}} \times 100$$

That Slope_{compound} solutions contained DHFR, test compound, NADPH, and DHF; Slope_{control} solutions contained DHFR, NADPH, and DHF; Slope_{blank} solutions contained NADPH and DHF only.

Subcellular localization

The cells were pretreated with **2a** (20 μM) in 2-cm dish then stained with LYSO tracker 2 h before and DAPI 30 min before **2a** was added then the supernatant was removed, washed with PBS for twice and the fluorescence was captured at 4 h and 8 h under fluorescence microscope ².

Wound-healing assay

HeLa cells (1.3×10^5 cells/well) were seeded in 6-well plate. After adherence, the medium was aspirated. Then the cell monolayers were scraped with a sterile micropipette tip in the central region to create a denuded zone with constant width. The cellular debris was washed with PBS (twice), and 2 ml of medium were added to each well, followed by treatment of 1 μM of **2a** (final concentration) or 4 Gy of X-ray or their combination. The wound closure of the HeLa cells was monitored and photographed at 0 and 24 h. The migrated cells were quantified by the pictures of the initial wounded monolayers comparing with that of the cells after incubation. Cells that migrated across the artificial lines were counted in 5 random cell fields. The cell migration effect was determined as a percentage (%) of the length of the migrated wound in comparison to the baseline value ³.

Antiproliferative Activity

Cell proliferation was measured using the MTT assay ⁴. HeLa cells were seeded in 96 well-plates at a density of 2×10^3 cells/well. Cells were irradiated with 4 Gy of X-ray alone or pre-incubated with different concentrations of **2a** (from 0.625 μM to 80 μM) for 6 hrs and then irradiated with a dose of 0 Gy or 4 Gy X-ray. As 72 h, 25 μl

of MTT (5 mg/ml) was added to each well and incubated for 3h. The supernatant was removed slowly and each well was added with 150 μ l of DMSO. The 96 well-plates were shaken gently on a shaker for 15 min then subjected to microplate reader recording absorbance at 570 nm. The cell viability was expressed as percentage of control.

Cellular uptake

HeLa cells were pre-seeded at the concentration of 5×10^5 cells/mL into 6-well plates. After 24 h, **2a** or **MTX** were added to the cells at the final concentration of 20 μ M and cells were incubated for 1/4, 1/2, 1, 2, 4 h respectively. Then the medium was removed and the cells were washed by PBS for three times to remove extra agents and were lysed with 200 μ L of 0.5% Tritonx-100. The concentrations of **2a** and MTX were measured by a microplate reader using the fluorescence intensity detection method (Ex: 396 nm, Em: 513 nm) and absorbance detection method (306 nm), respectively.

Intracellular ROS lever

The intracellular ROS lever was determined by means of a red fluorescent probe: DHE ⁵. Cells received different treatment (4 Gy of X-ray, **2a** or their combination) were loaded with DHE (10 μ M) and incubated at 37 °C. The cells were washed twice with PBS. The fluorescence intensity (red channel) and fluorescence value (λ_{ex} : 535, λ_{em} : 630) were obtained from an imaging reader (Cytation 5, Biotek). Cells received no treatment were used as a control.

Flow cytometric analysis

HeLa cells were treated with **2a** (1 μ M) for 6 h and then were exposed to 4 Gy of X-ray irradiation or not, and further incubated for another 24 h. Then cells were harvested by trypsinization, centrifuged to remove supernatant and washed with PBS. The cells were subsequently fixed in 3 ml of ethanol (75%) overnight at -20 °C. Then the ethanol was removed, and the cells were washed with PBS and stained with

propidium iodide (PI) for 30 min at 37 °C. Stained cells were analyzed using a flow cytometer⁶. In all cases at least 10,000 live events were collected for analysis.

Mitochondrial Morphology

The HeLa cells were seed on 2-cm glass petri dishes at a density of 1×10^5 cells/ml. The adherent cells were treated with 1 μ M of **2a** or 4 Gy of X-ray or their combination. After incubation at 37 °C for 24 h, the cells were washed with PBS for twice and stained with Mitotracker (red) for 1.5 h and then DAPI for 30 min, followed by washing out the probes and observing under a microscope (EVOSs FL Auto Imaging System)⁷.

Mitochondrial Membrane Potential ($\Delta\Psi$ m)

Cells cultured in 6-cm dish (1.2×10^5 cells/ml) were treated with 1 μ M **2a** or 4 Gy X-ray or their combination. After treatment for 24 h, the cells were trypsinized and resuspended in 400 μ l of PBS containing 10 μ g/mL JC-1. Then the supernatant was removed after incubation for 30 min. Cell pellets were re-suspended in PBS and analyzed by flow cytometry⁸. The percentage of green fluorescence from JC-1 monomers represented the cells that lost $\Delta\Psi$ m.

Caspases activity assay

Cells (1×10^6 cells/dish) were seeded in 6 cm dishes. After treated with X-ray (4 Gy) or **2a** (1 μ M) alone or their combination, cells were harvested and lysed by RIPA buffer. Cell lysates were centrifugated at 12000 rpm for 5 min and then remove the precipitate. The remained clear lysates were used for protein concentration and caspase activity measurement. Briefly, total protein (70 μ g /well) were placed in 96-well plates, followed by adding 3 μ l specific caspase substrates (Ac-DEVD-AMC for caspase-3, Ac-IETD-AMC for caspase-8 and Ac-LEHD-AMC for caspase-9). Plates were incubated at 37°C for 2h under dark condition and caspase activity was determined by fluorescence intensity with the corresponding excitation and emission wavelengths (380 and 440 nm).

Western blot analysis

Cells were firstly treated with **2a**, X-ray or their combination, then the medium was removed and the cells were washed with PBS, lysed in ice-cold RIPA buffer. The protein concentrations were determined by BCA protein assay kit. Each extract (60 μ g protein) was fractionated by electrophoresis and transferred to a PVDF membrane. The membranes were subsequently blocked with milk for 2 h, and then incubated with primary antibodies overnight at 4 °C. Then the membranes were washed using TBST and were subjected to the secondary antibody for 1.5 h. After washed with TBST for three times, the bands were visualized by incubation with HRP substrate and recorded⁹.

***In vivo* anti-tumor analysis of 2a**

The *in vivo* anti-tumor activity and radiosensitization of **2a** were tested by nude mice model. The animal experiments were approved by the Laboratory Animal Ethics Committee of Jinan University. Female Balb/c nude mice (n=20, 4-week old) were purchased from Guangdong Medical Laboratory Animal Center. The mice were injected subcutaneously with 1×10^6 HeLa cells in 100 μ L PBS. After one week and the tumor volumes were about 100 mm³, the mice were assigned randomly into four groups: Control, **2a**, 4G and **2a**+4G. Administration of **2a** was through tail intravenous injection every three days at a dose of 4 mg/kg. X-ray treatment was conducted at the same time with a dose of 4 Gy. The mice of control group received equal volume of PBS during the 21-day treatment period. The body weight and tumor volume of the mice were measured every time when they received treatments.

Pathology analysis

The main organs and tumor of mice were fixed in 4% paraformaldehyde followed by paraffin embedment and hematoxylin and eosin staining¹⁰. The H&E and immunohistological chemistry analysis was obtained using a digital light microscope (NIKON, Eclipse Ni-U).

Hematology analysis of HeLa xenograft nude mice

The blood samples were collected from eyeballs, and about 500 μ L serums was obtained by centrifugation, which was sent to the blood testing center of the first affiliated hospital of Jinan University for Blood Biochemical Indexes Analysis¹¹. The analysis indexes included glutamic pyruvic transaminase (ALT); Aspartate aminotransferase (AST), uric acid (UA) and BUN (blood urea nitrogen).

Pharmacokinetics analysis

The pharmacokinetics analysis was performed as previous reported method [12]. Three female rats (\geq 250 g) were purchased from Guangdong Medical Laboratory Animal Center. The compound **2a** were administrated through intravenous injection at a dose of 1 mg/kg. Blood samples were collected via the ophthalmic venous plexus at 0, 5, 15, 30 min and 1, 2, 4, 8, 24 and 48 h. After standing at room temperature for 30 min, the blood samples were centrifuged at 3000 rpm for 5 min to collect serums. To extract **2a**, 150 μ l of serum were mixed with 300 μ l n-butyl alcohol by vortex blending for 1 min. After centrifuge at 10000 rpm for 1 min, 100 μ l of extraction were added to 96-well plate and the concentration of **2a** were measured by recording the fluorescent intensity at the excitation wavelength of 396 nm and the emission wavelength of 513 nm.

Statistical analysis

All experiments were carried out in triplicate ($n = 3$) and results were expressed as mean \pm SD. Difference between two groups was analyzed by two-tailed Student's-t test. Difference of multiple groups was analyzed by one unpaired multiple *t*-test. Difference with $P < 0.05$ (*) or $P < 0.01$ (**) was considered statistically significant.

References

1. Singla, P.; Luxami, V.; Paul, K., Synthesis, in vitro antitumor activity, dihydrofolate reductase inhibition, DNA intercalation and structure-activity

relationship studies of 1,3,5-triazine analogues. *Bioorg Med Chem Lett* **2016**, *26*(2), 518-523.

2. Luo, J.; Liu, Q. Y.; Morihiro, K.; Deiters, A., Small-molecule control of protein function through Staudinger reduction. *Nat Chem* **2016**, *8*(11), 1027-1034.

3. Su, S. C.; Liao, J. Y.; Liu, J.; Huang, D.; He, C. H.; Chen, F.; Yang, L. B.; Wu, W.; Chen, J. N.; Lin, L.; Zeng, Y. J.; Ouyang, N. T.; Cui, X. Y.; Yao, H. R.; Su, F. X.; Huang, J. D.; Lieberman, J.; Liu, Q.; Song, E. W., Blocking the recruitment of naive CD4(+) T cells reverses immunosuppression in breast cancer. *Cell Res* **2017**, *27*(4), 461-482.

4. Liang, Y. W.; Zheng, J. S.; Li, X. L.; Zheng, W. J.; Chen, T. F., Selenadiazole derivatives as potent thioredoxin reductase inhibitors that enhance the radiosensitivity of cancer cells. *Eur J Med Chem* **2014**, *84*, 335-342.

5. You, Y. Y.; He, L. Z.; Ma, B.; Chen, T. F., High-Drug-Loading Mesoporous Silica Nanorods with Reduced Toxicity for Precise Cancer Therapy against Nasopharyngeal Carcinoma. *Adv Funct Mater* **2017**, *27*(42), 201703313.

6. Liang, Y. W.; Zhou, Y. L.; Deng, S. L.; Chen, T. F., Microwave-Assisted Syntheses of Benzimidazole-Containing Selenadiazole Derivatives That Induce Cell-Cycle Arrest and Apoptosis in Human Breast Cancer Cells by Activation of the ROS/AKT Pathway. *Chemmedchem* **2016**, *11*(20), 2339-2346.

7. Kuntz, E. M.; Baquero, P.; Michie, A. M.; Dunn, K.; Tardito, S.; Holyoake, T. L.; Helgason, G. V.; Gottlieb, E., Targeting mitochondrial oxidative phosphorylation eradicates therapy-resistant chronic myeloid leukemia stem cells. *Nat Med* **2017**, *23*(10), 1234-1240.

8. Lee, D. G.; Choi, B. K.; Kim, Y. H.; Oh, H. S.; Park, S. H.; Bae, Y. S.; Kwon, B. S., The repopulating cancer cells in melanoma are characterized by increased mitochondrial membrane potential. *Cancer Lett* **2016**, *382*(2), 186-194.

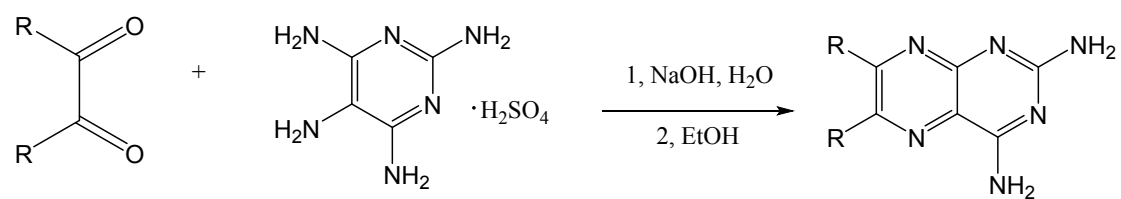
9. Duncombe, T. A.; Kang, C. C.; Maity, S.; Ward, T. M.; Pegram, M. D.; Murthy, N.; Herr, A. E., Hydrogel Pore-Size Modulation for Enhanced Single-Cell Western Blotting. *Adv Mater* **2016**, *28*(2), 327-334.

10. Peters, I. T. A.; Stegehuis, P. L.; Peek, R.; Boer, F. L.; van Zwet, E. W.; Eggermont, J.; Westphal, J. R.; Kuppen, P. J. K.; Trimbos, J. B.; Hilders, C. G. J. M.; Lelieveldt, B. P. F.; van de Velde, C. J. H.; Bosse, T.; Dijkstra, J.; Vahrmeijer, A. L., Noninvasive Detection of Metastases and Follicle Density in Ovarian Tissue Using Full-Field Optical Coherence Tomography. *Clinl Cancer Res* **2016**, *22*(22), 5506-5513.

11. Iraci, N.; Gaude, E.; Leonardi, T.; Costa, A. S. H.; Cossetti, C.; Peruzzotti-Jametti, L.; Bernstock, J. D.; Saini, H. K.; Gelati, M.; Vescovi, A. L.; Bastos, C.; Faria, N.; Occhipinti, L. G.; Enright, A. J.; Frezza, C.; Pluchino, S., Extracellular vesicles are independent metabolic units with asparaginase activity. *Nat Chem Biol* **2017**, *13*(9), 951-955.

12. T.Y. Seiwert, J.K. Salama, E.E. Vokes, The concurrent chemoradiation paradigm—general principles, *Nat. Clin. Pract. Oncol.* **2007**, *4*, 86.

Synthetic route of Compounds



Scheme S1. Synthetic route of 2,4-diaminopteridine derivatives.

Supplementary figures

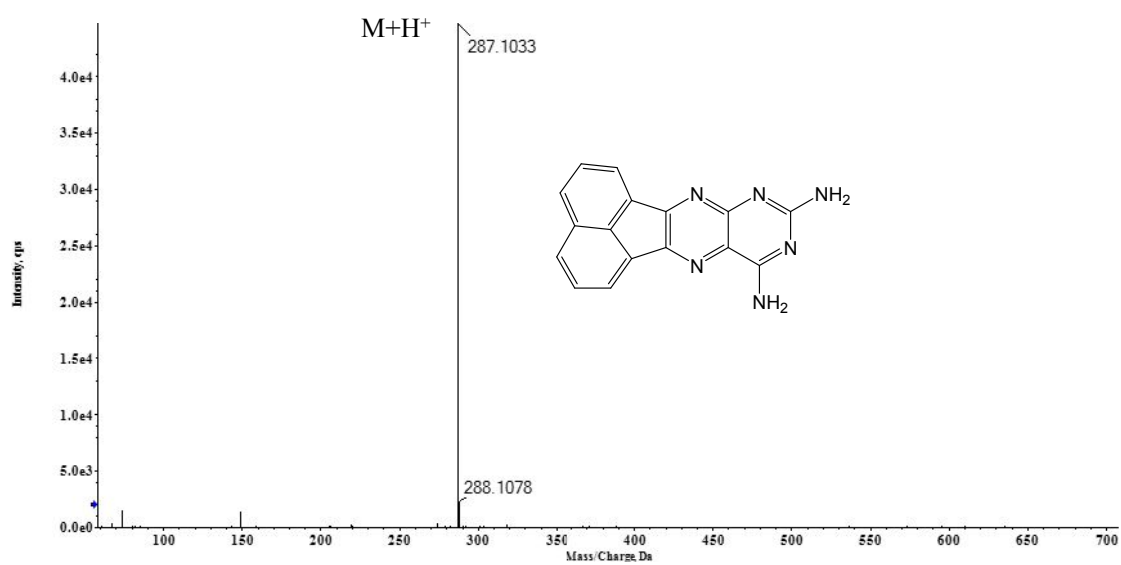


Figure S1. HRMS of **2a**

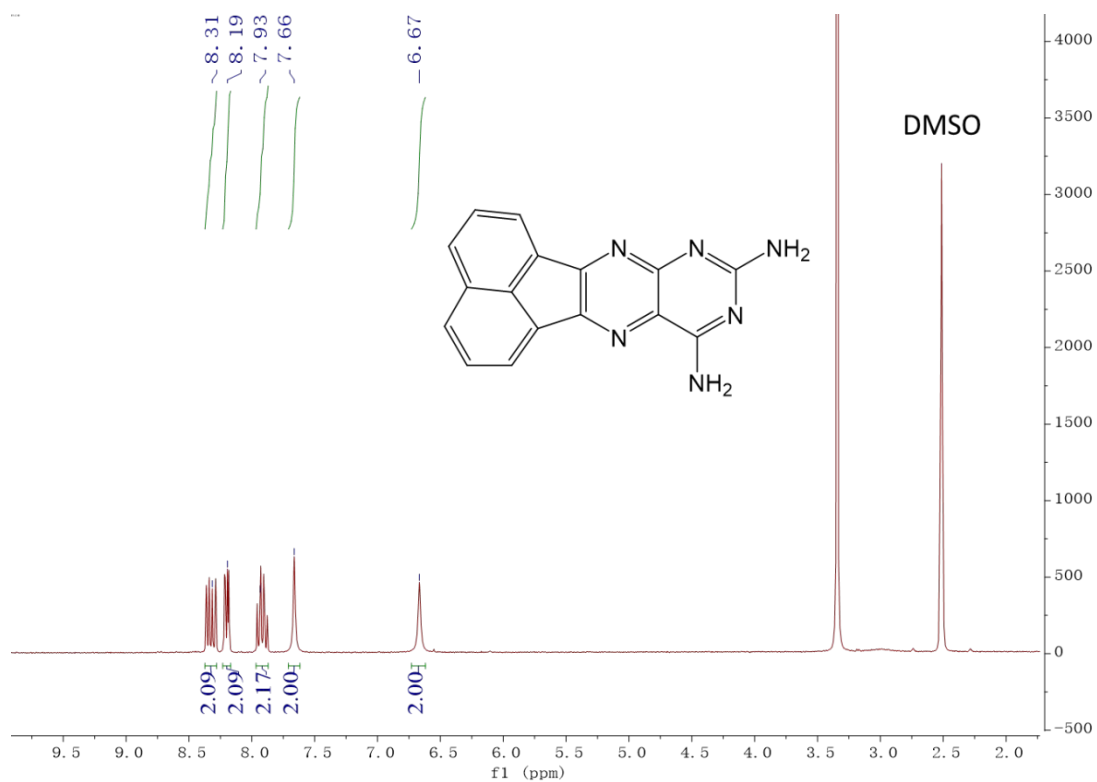


Figure S2. ^1H NMR (DMSO- d_6) of **2a**.

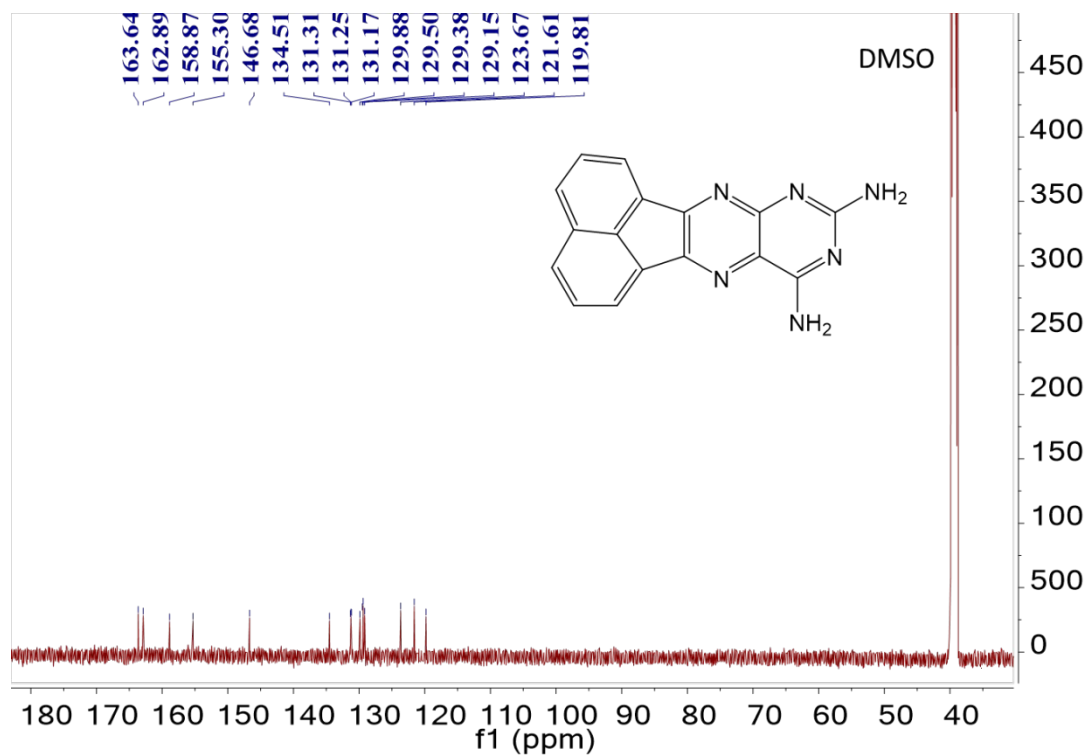


Figure S3. ^{13}C NMR (DMSO- d_6) of **2a**.

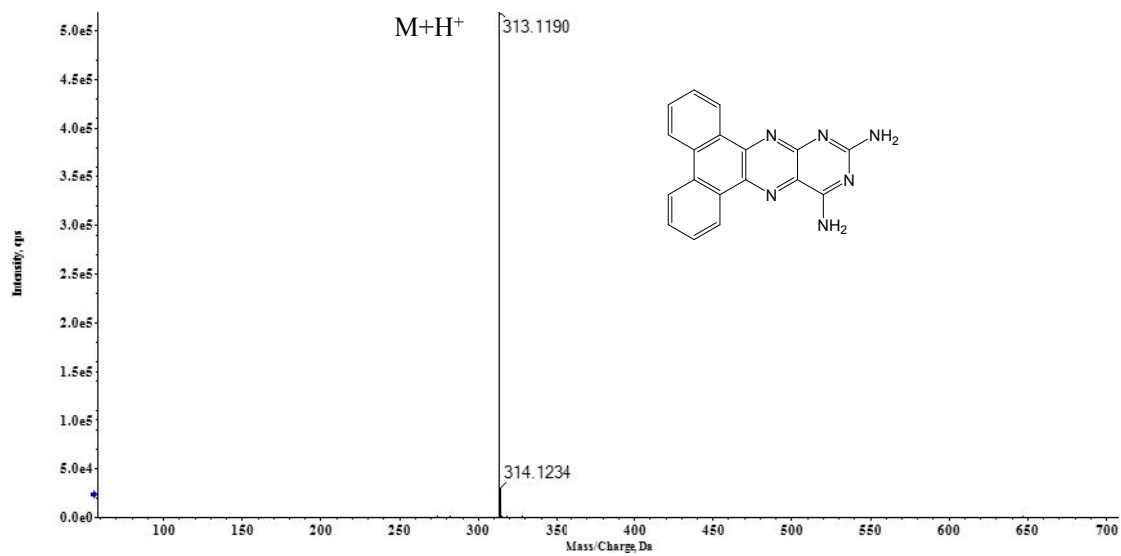


Figure S4. HRMS of **2b**.

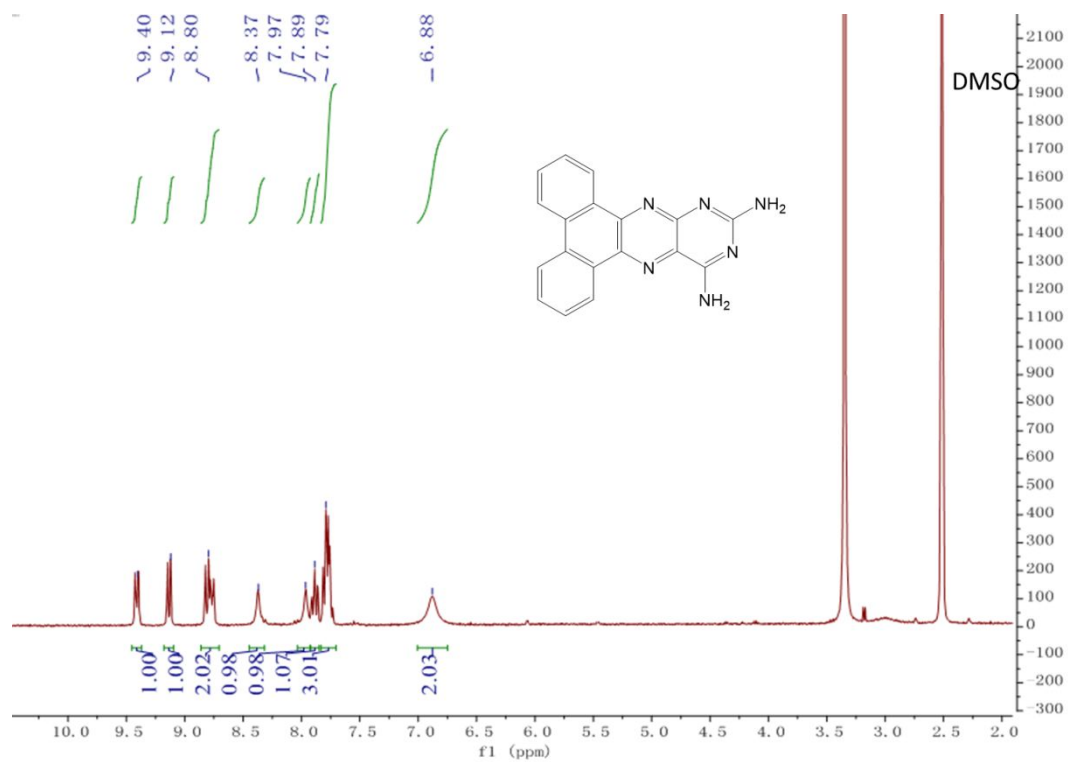


Figure S5. ¹H NMR (DMSO-*d*₆) of **2b**.

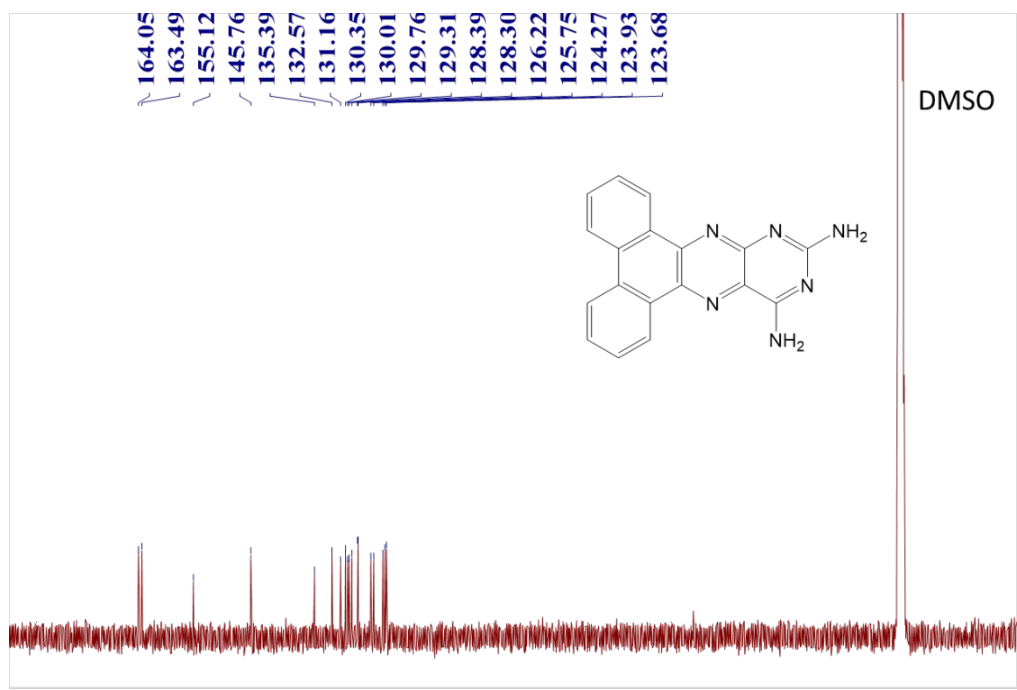


Figure S6. ^{13}C NMR (DMSO-*d*₆) of **2b**.

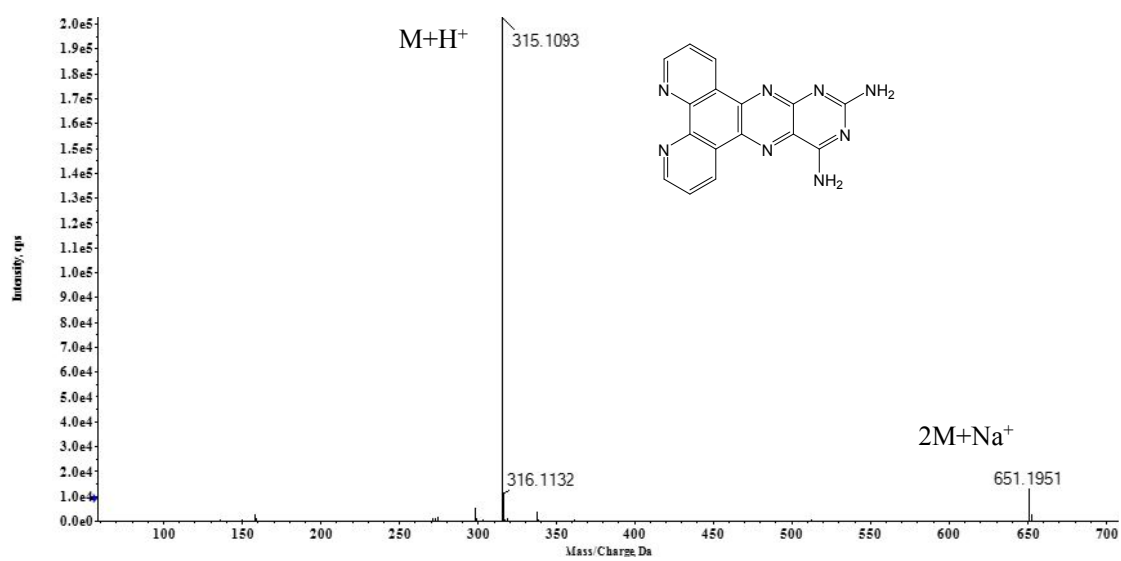


Figure S7. HRMS of **2c**.

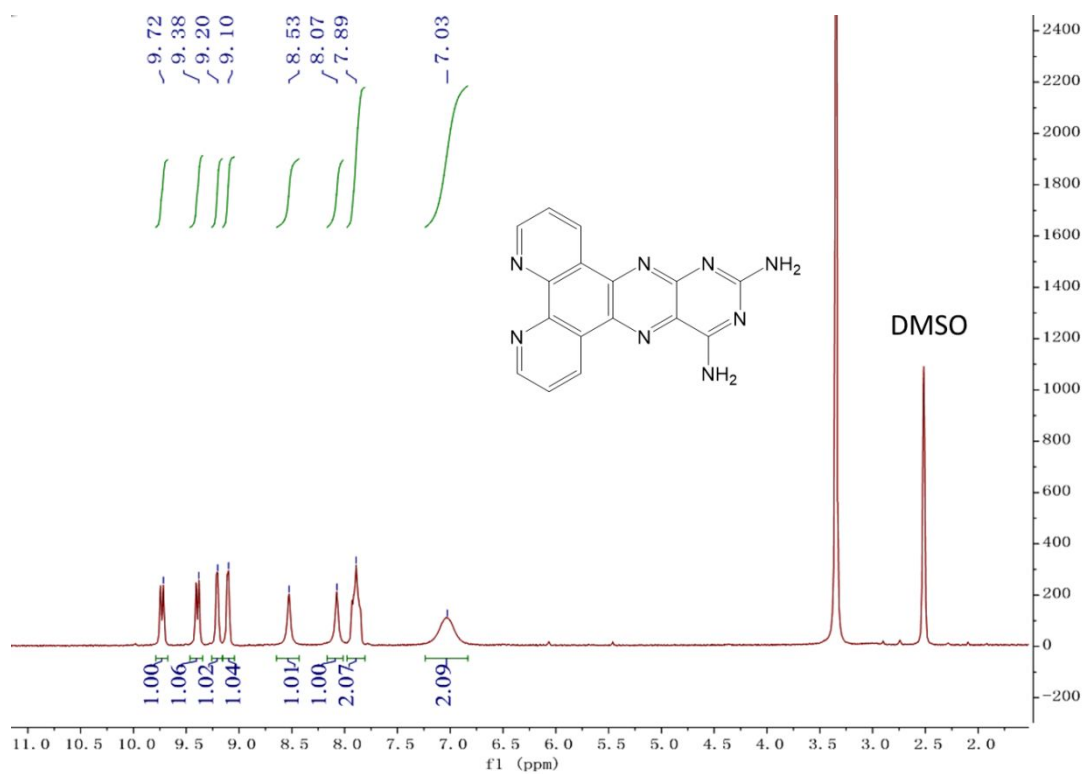


Figure S8. ^1H NMR (DMSO- d_6) of **2c**.

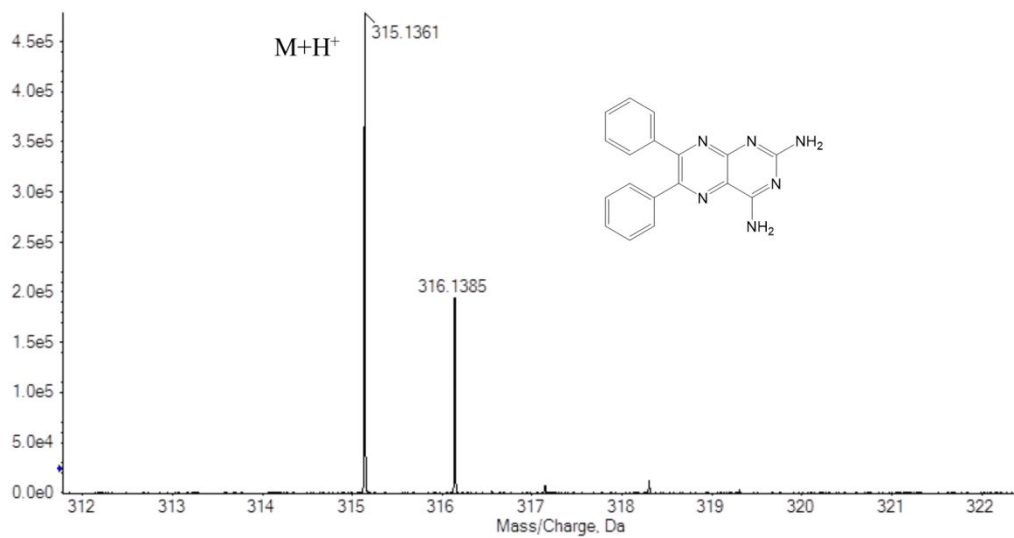


Figure S9. HRMS of **2d**.

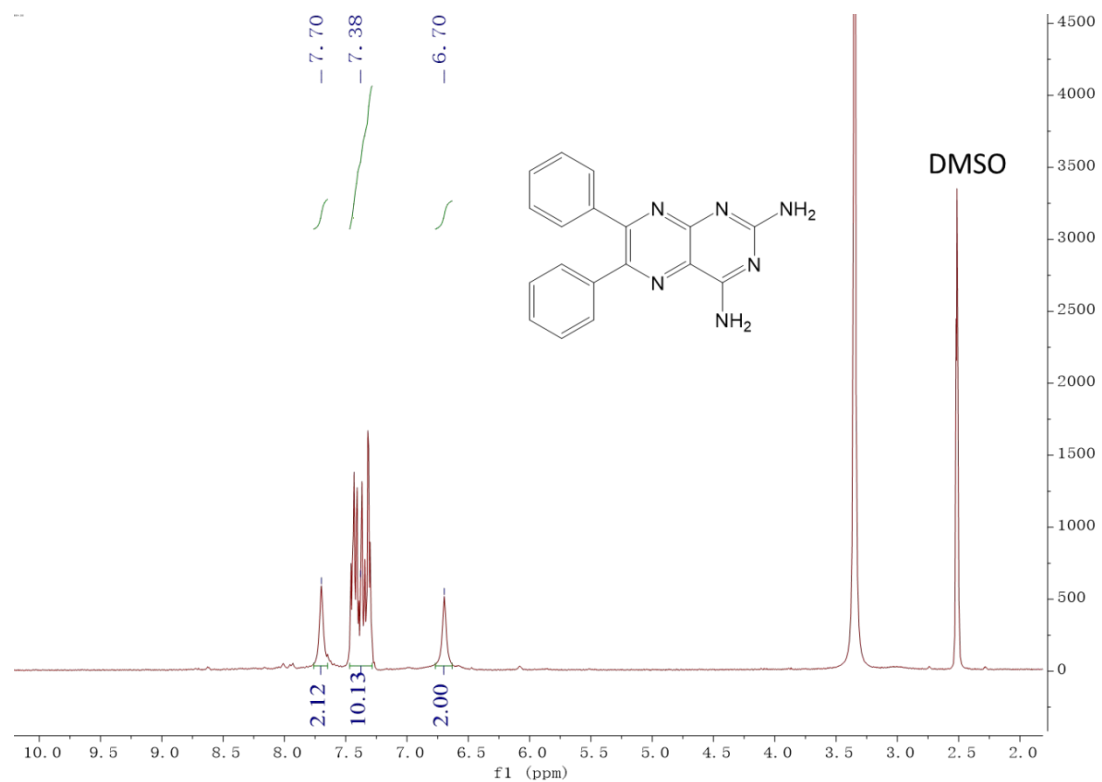


Figure S10. ¹H NMR (DMSO-*d*₆) of **2d**.

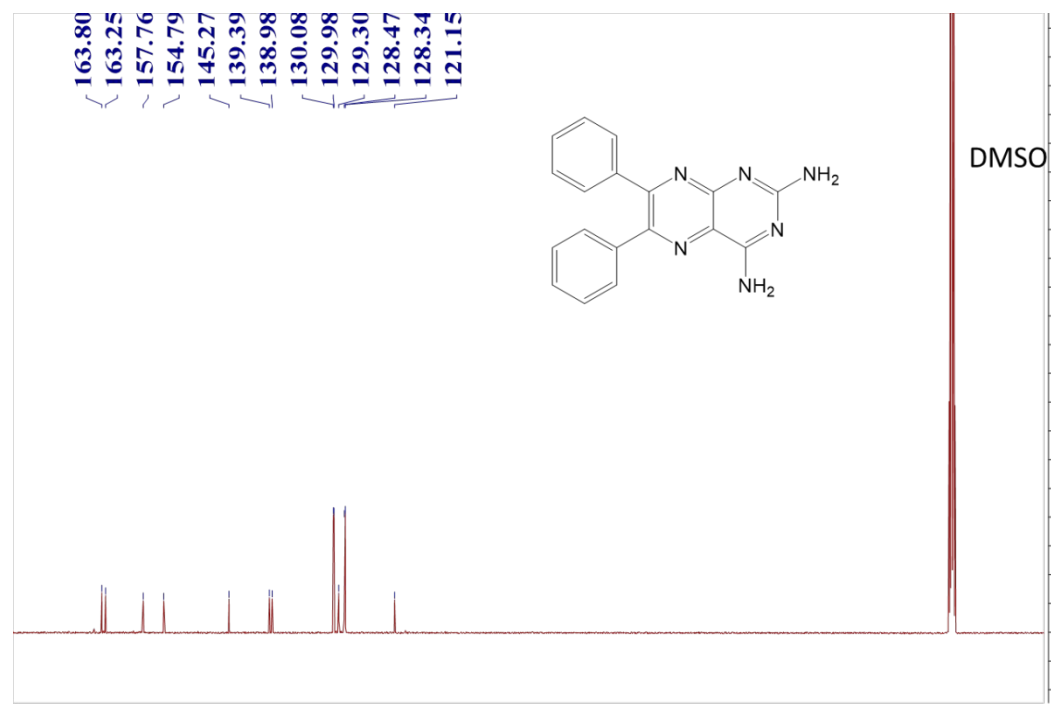


Figure S11. ¹³C NMR (DMSO-*d*₆) of **2d**.

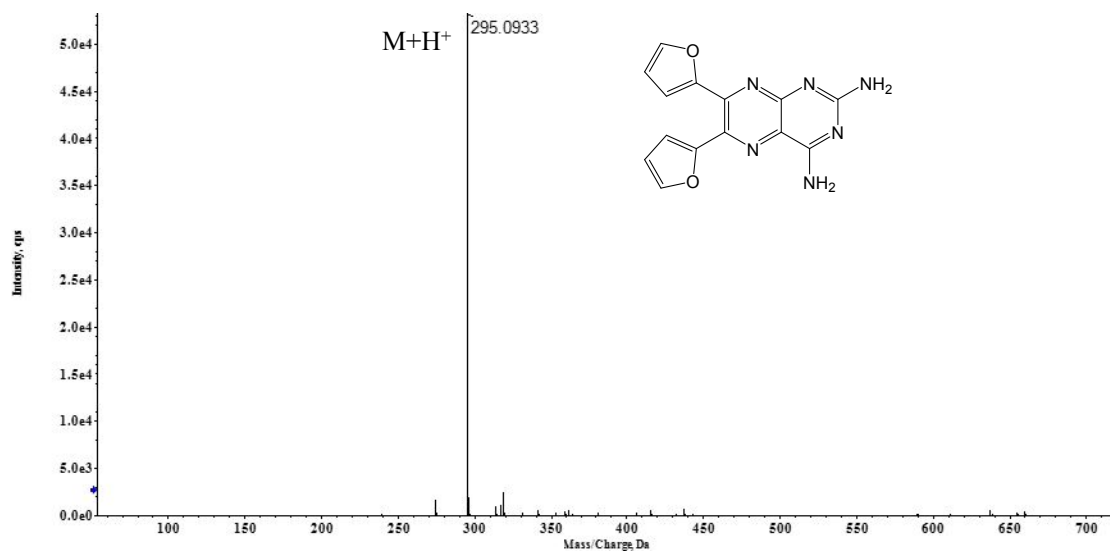


Figure S12. HRMS of **2e**.

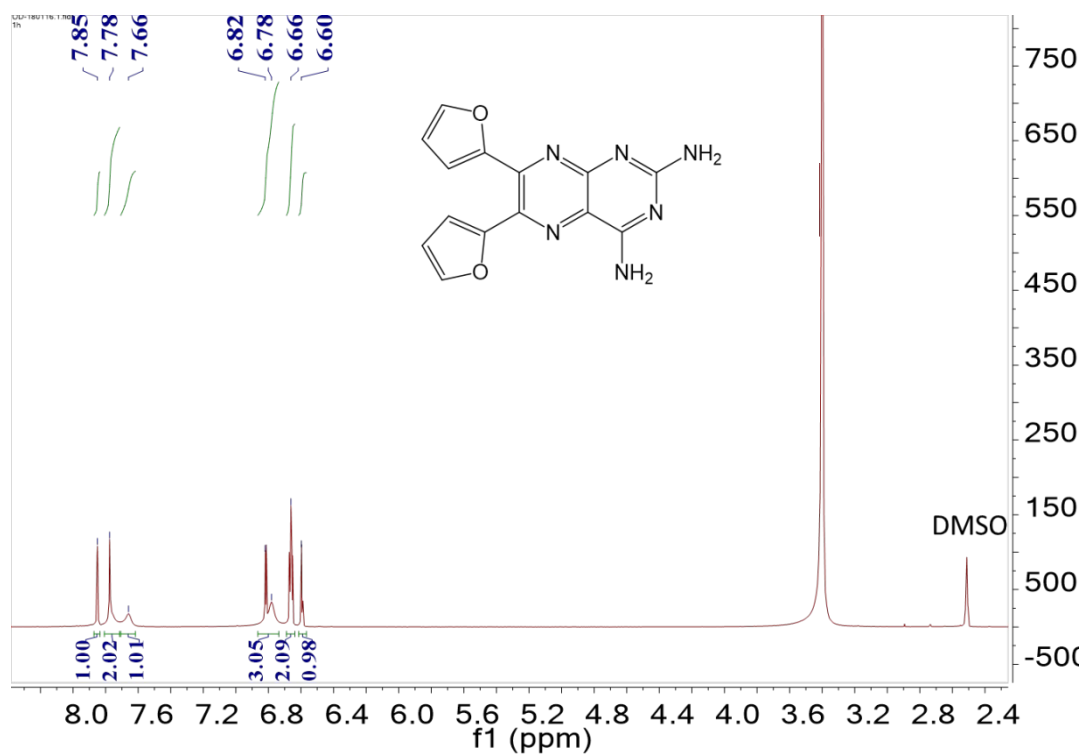


Figure S13 ¹H NMR (DMSO-*d*₆) of **2e**.

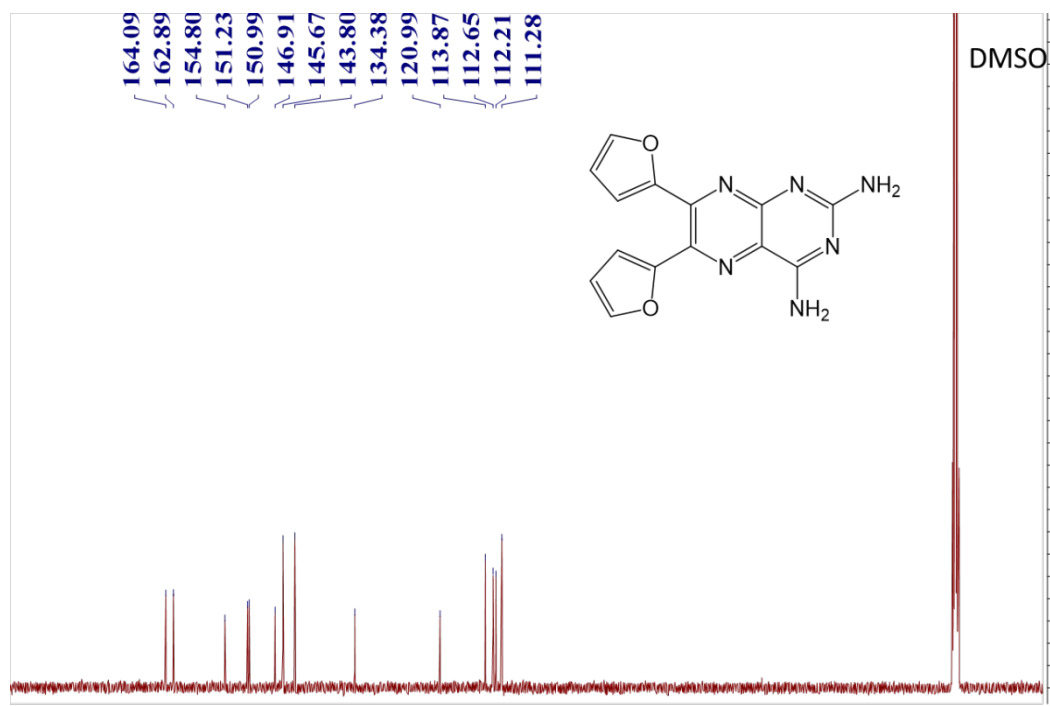


Figure S14 ^{13}C NMR (DMSO-*d*₆) of **2e**.

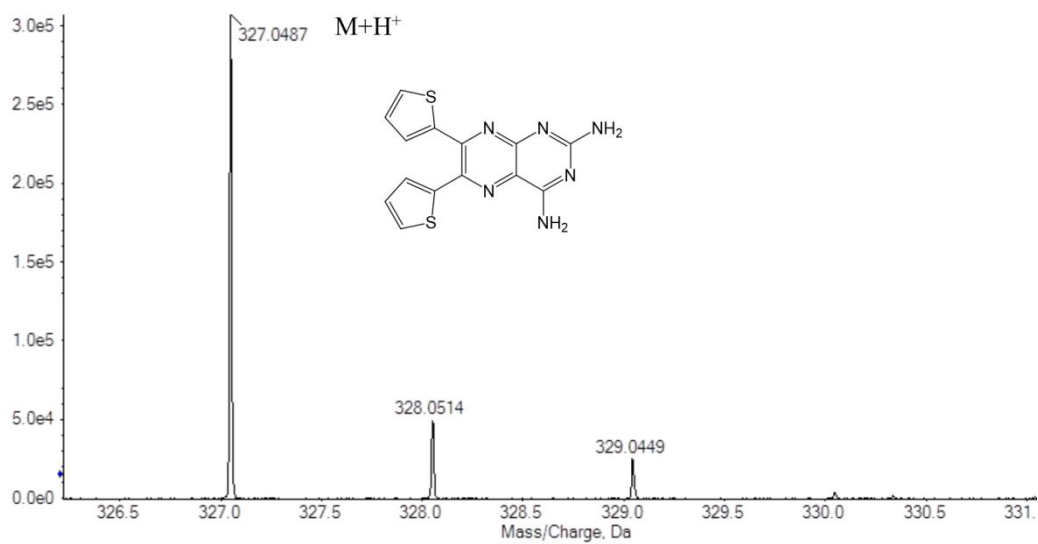


Figure S15. HRMS of **2f**.

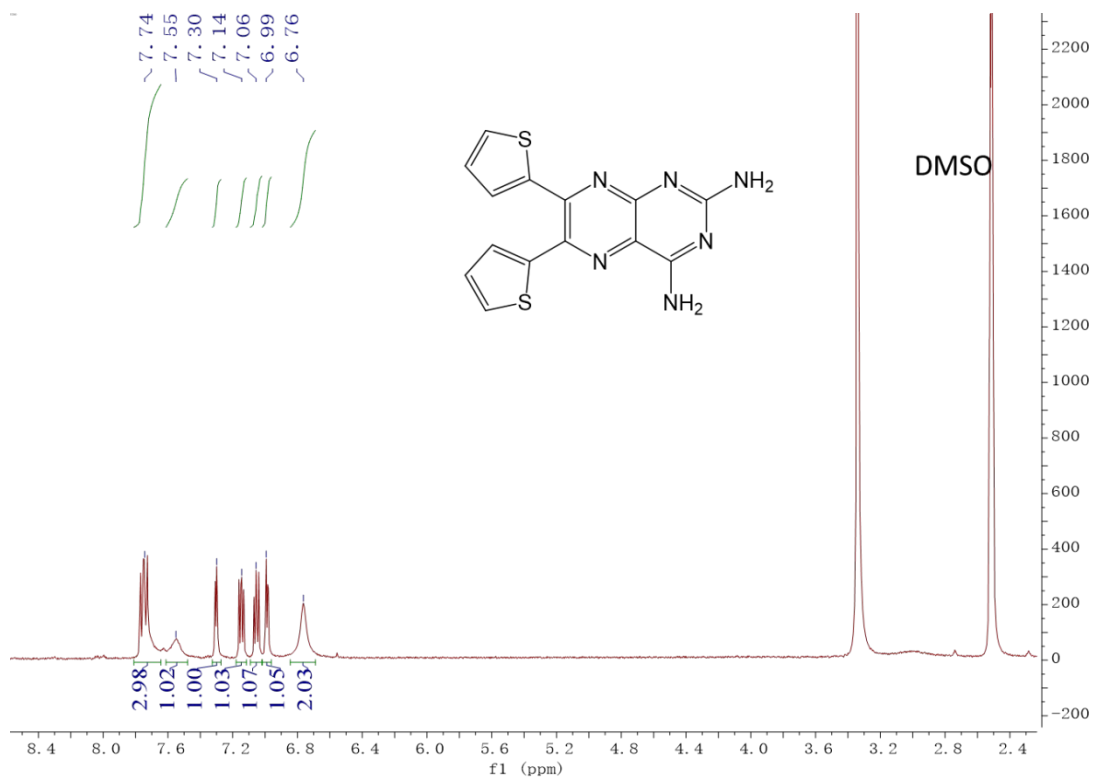


Figure S16. ¹H NMR (DMSO-*d*₆) of **2f**.

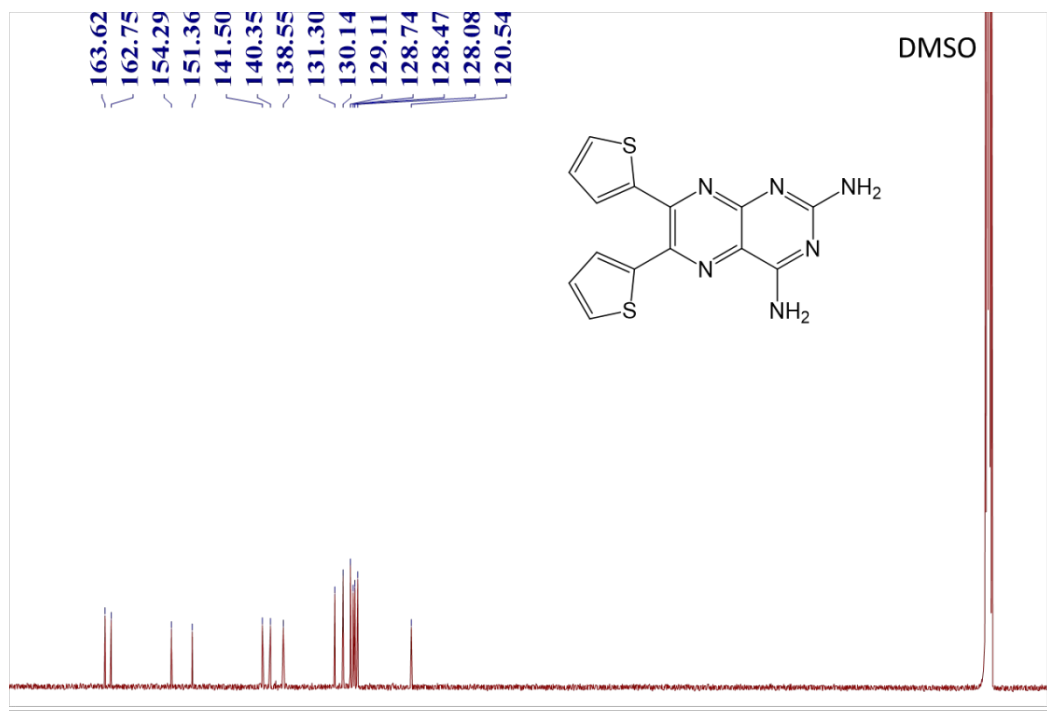


Figure S17. ¹³C NMR (DMSO-*d*₆) of **2f**.

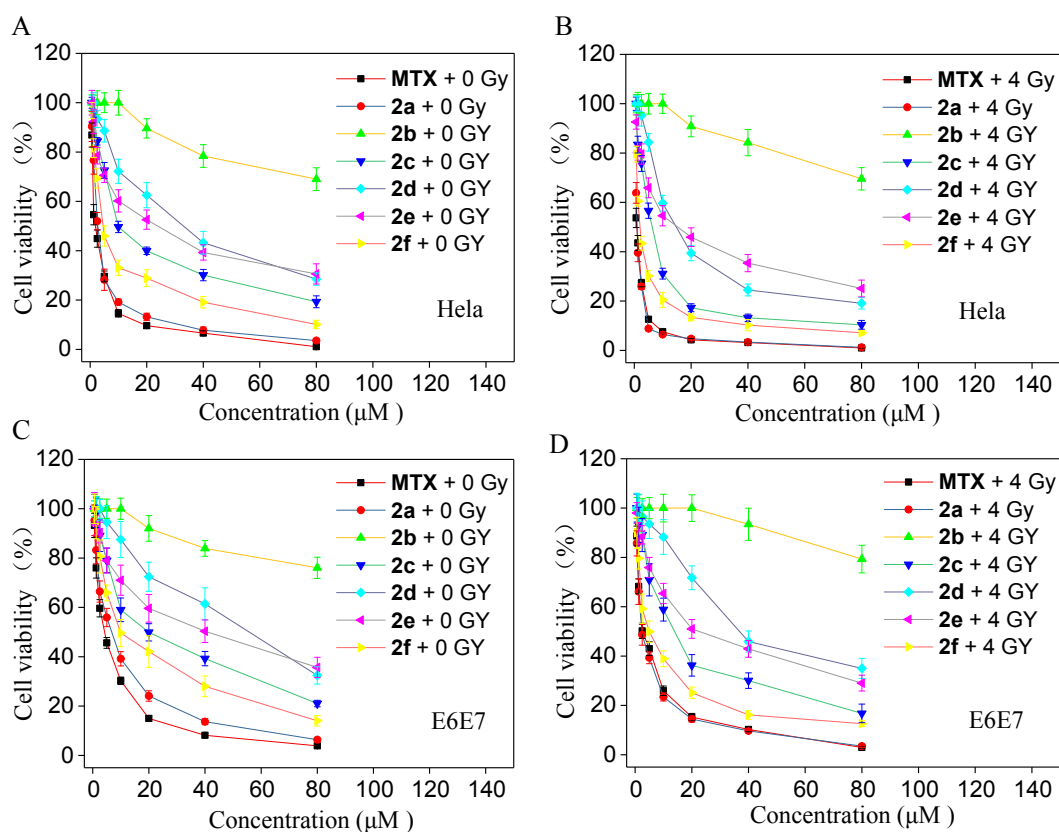


Figure S18. Compounds **1a**, **1b**, **1c**, **1d**, **1e** and **1f** treatment effects on Hela cells with or without 4 Gy irradiation. Anti-proliferation activity of **1a**, **1b**, **1c**, **1d**, **1e** and **1f** on Hela cells (A), (B) and E6E7 cells (C), (D). Cells were treated with increasing concentrations of compounds for 12 h then were unexposed or exposed to 4 Gy irradiation and incubated for further 60 h. Cell viability was determined by MTT assay.

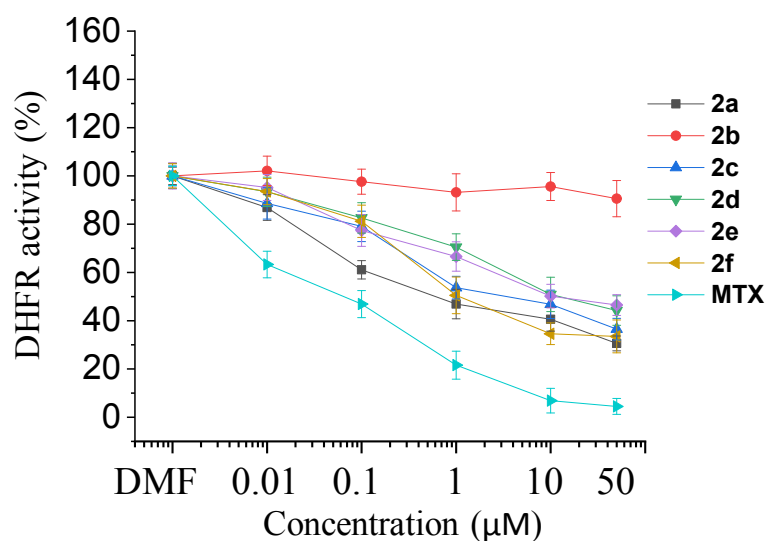


Figure S19. The DHFR inhibitory activity of compound **2a-2f** and MTX. In 96-well plate containing a solution of 20 μM dihydrofolate (DHF), 5×10^{-2} units of recombinant human DHFR and different concentrations of 2,4-diaminopteridine derivatives in 0.05 M phosphate buffer (containing 2% DMF), a final concentration of 200 μM NADPH was added to initiate the systematic reaction.

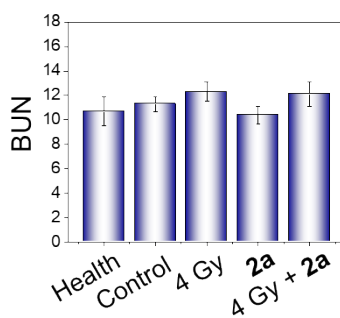


Figure S20. Blood biochemistry analysis of BUN (blood urea nitrogen) in mice after different treatment.

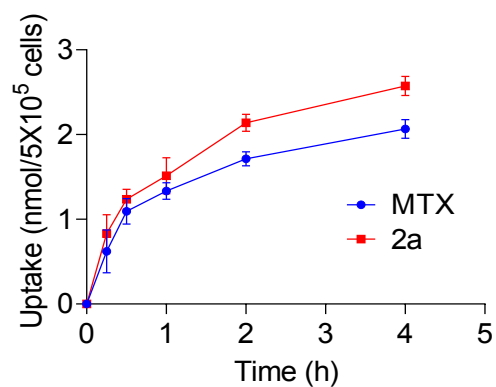


Figure S21. Uptake of MTX and **2a** by Hela cells. Cells were incubated with MTX or **2a** (4 μ M) for 0 to 4 h and were determined by fluorescence intensity.

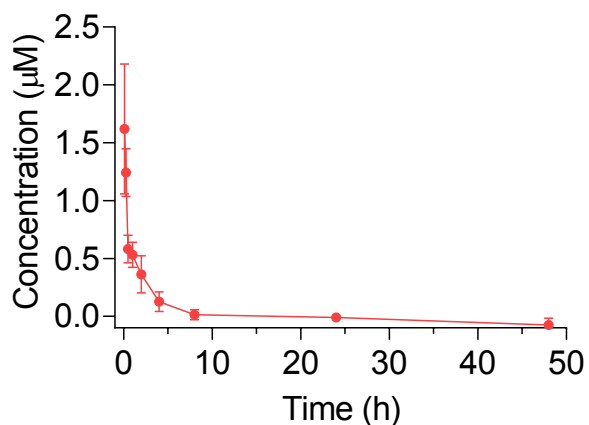


Figure S22. Pharmacokinetic parameters of **2a** after injection.

Table S1. Analysis of $t_{1/2\beta}$, elimination phase and half-life period of **2a**.

Compound	$t_{1/2\beta}$ (h)	AUC _{0-48 h} (μ mol/L*h)	C _{max} (μ mol/L)	Cl (mg)/(μ mol/L)/h	MRT _{0-inf} (h)
2a	1.37 \pm 0.58	2.1 \pm 0.82	1.62 \pm 0.56	0.13 \pm 0.06	1.76 \pm 0.03

AUC_{0-48 h}, area under the concentration versus time curve (0-48 h). C_{max}, maximum concentration observed. Cl, clearance of medicine. MRT, mean retention time.